Generalized Flory–Huggins Model for Heat-of-Mixing and Phase-Behavior Calculations of Polymer–Polymer Mixtures

M. TAIMOORI,[1] H. MODARRESS,[1] G. A. MANSOORI[2]

[1] Department of Chemical Engineering, Amir Kabir Technical University, No. 424, Hafez Avenue, Tehran, Iran

[2] Department of Chemical Engineering, University of Illinois at Chicago, 810 South Clinton, Chicago, Illinois 60607-7000

Received 20 September 1999; accepted 14 January 2000

ABSTRACT: An extended and generalized Flory–Huggins model for calculating the heats of mixing and predicting the phase stability and spinodal diagrams of binary polymer–polymer mixtures is presented. In this model, the interaction parameter is considered to be a function of both temperature and composition. It is qualitatively shown that the proposed model can calculate the heats-of-mixing curves containing exothermic, endothermic, and S-shaped or sigmoidal types and predict the spinodals, including the upper and lower critical solution temperatures, and closed-loop miscibility regions. Using experimental results of analog calorimetry for four polymer mixtures of polystyrene/poly(vinyl chloride) (PS/PVC), polycarbonate (PC)/poly(ethylene adipate) (PEA), polystyrene/poly(vinyl acetate) (PS/PVAc), and ethylene vinyl acetate copolymer (EVA Co)/chlorinated polyethylene (CPE), the capabilities of the proposed functionality for the interaction parameter was studied. It is shown that this function can be used satisfactorily for the heat-of-mixing calculations and phase-behavior predictions. © 2000 John Wiley & Sons, Inc. J Appl Polym Sci 78: 1328–1340, 2000

Key words: polymer solutions; polymer mixtures; Flory–Huggins; phase stability; interaction parameter

INTRODUCTION

In polymer research, many studies have been devoted to the study of phase behavior and the miscibility of polymer mixtures. Phase behavior and miscibility regions of these mixtures are determined by spinodal-phase diagrams. In the field of polymer miscibility, undoubtedly, the pioneering work of Flory[1–3] and Huggins[4,5] (FH) presents the most familiar theory for predicting phase behavior and spinodal curves. The interaction parameter in the original version of the FH theory was assumed to be independent of the mixture composition. Because of its simplicity, this theory is widely used to predict phase-separation phenomena in binary polymer solutions and mixtures. Much research has been done to improve the shortcomings of the original FH theory, among which we can mention the recent works of Koningsveld et al.,[6,7] Painter et al.,[8,9] and other workers.[10,11]

There are a number of other theories such as the equation of state,[12–17] corresponding states,[18] and group contribution[19] which have been employed for phase-behavior predictions in multicomponent polymer systems. Usually, pure component characteristic properties, which are required by these models for phase-stability studies, are not available and therefore employing these models is limited to some particular cases.

Correspondence to: H. Modarress.

Journal of Applied Polymer Science, Vol. 78, 1328–1340 (2000)

On the other hand, there are considerable experimental data about temperature and composition dependency of the interaction parameters in polymer–solvent and polymer–polymer systems.[20–22] Various experimental methods can be used to determine the composition and temperature dependency of the interaction parameter such as osmotic pressure,[23] light scattering,[23] and calorimetric measurements.[24] Thus, it seems that using these experimental data and fitting an empirical form of the interaction parameter can produce exact results for predicting the thermodynamic functions and phase behavior of polymer systems.

In the present work, the basic FH lattice theory is generalized by introducing an empirical expression for its interaction parameter, which is dependent on the temperature and mixture composition. The form of this expression is a combination of temperature and composition terms with five constant coefficients. Evaluation of these coefficients is made by using experimental heat of mixing data. The presented method can be used to calculate the enthalpy of mixing and the miscibility or phase stability of polymer mixtures.

THEORY AND MODEL DESCRIPTION

To illustrate the stability of a binary polymer mixture, we must consider the Gibbs free-energy change of mixing versus mixture composition. A negative free energy of mixing is a necessary but not sufficient condition for phase stability or the miscibility of components. In a two-component polymer system at a given temperature and pressure, phase stability is defined by the following condition:

$$\frac{\partial^2 \Delta G^{\text{mix}}}{\partial \varphi^2} > 0 \tag{1}$$

where ΔG^{mix} is the Gibbs free-energy change upon mixing and φ is the volume fraction.

In the original FH[1–5] lattice theory, the following relation was obtained for the Gibbs free energy of mixing:

$$\frac{\Delta G^{\text{mix}}}{RT} = \frac{\varphi_1}{r_1} \ln \varphi_1 + \frac{\varphi_2}{r_2} \ln \varphi_2 + \chi \varphi_{\text{FH}} \varphi_1 \varphi_2 \tag{2}$$

where r_1 and r_2 are the number of chain segments for two components; and R and T, the universal gas constant and temperature, respectively; and χ_{FH}, the FH interaction parameter. According to FH lattice theory, each lattice site is occupied by a segment. For polymer mixtures, an arbitrary reference volume is chosen for the system as the lattice cell volume and the number of chain segments for each component is obtained as follows:

$$r_i = \frac{V_i}{\nu_{\text{ref}}} = \frac{M_i \nu_i}{\nu_{\text{ref}}} \quad (i = 1, 2) \tag{3}$$

where V_i and M_i are the molar volume and molecular weight of "ith" component; ν_{ref}, the reference lattice cell molar volume; and ν_i, the specific volume of "ith" component.

The FH interaction parameter is defined as[25]

$$\chi_{\text{FH}} = \frac{z \Delta w_{12}}{RT} \tag{4}$$

where z is the coordination number of the lattice and Δw_{12} is the change in energy for the formation of an unlike contact pair 1–2 between the segments of the first and second components from two like contact pairs of 1–1 and 2–2. The term $z\Delta w_{12}$ in eq. (4) is the energy associated with mixing of the polymer segments and is considered to be independent of temperature variations.

In eq. (2), the two logarithmic terms represent the combinatorial entropy contribution to mixing. The third term contributes to the heat effects due to the interaction energy between the segments of the two components. According to eq. (2), the enthalpy of mixing is obtained as follows:

$$\frac{\Delta H^{\text{mix}}}{RT} = \chi_{\text{FH}} \varphi_1 \varphi_2 \tag{5}$$

From eqs. (4) and (5), it is evident that the original FH theory gives an enthalpy of mixing which is independent of temperature. Experimental results for various mixtures show that this is not generally true and ΔH^{mix} must be a function of temperature.[26–31]

On the other hand, it is known that molecular interactions among polymer segments can lead to the reorientation of the molecules in the mixture, which differ from the orientation of molecules in their pure state. Therefore, it was postulated by Flory[25] that a contribution to the entropy of mix-

ing should be considered which comes from segment–segment interactions and was named the noncombinatorial entropy of mixing. According to this interpretation, the FH interaction parameter, χ_{FH}, must be substituted by a temperature- and composition-dependent interaction parameter, χ, which is written as the sum of two parts: one part for the enthalpic effect, χ_H, which is due to the energy change upon mixing, and the other part for the entropic effect, χ_S, which is due to noncombinatorial entropy:

$$\chi = \chi_H + \chi_S \tag{6}$$

where χ_H and χ_S are defined as[25]

$$\chi_H = -T\left(\frac{\partial \chi}{\partial T}\right)_{\varphi_2} \tag{7}$$

$$\chi_S = \left(\frac{\partial (\chi T)}{\partial T}\right)_{\varphi_2} \tag{8}$$

It is worth noting that upon substituting eq. (4) into eq. (8) we have $\chi_S = 0$ and, therefore, the noncombinatorial entropy contribution cannot be taken into account, while for some polymer–polymer systems, it was observed experimentally that the noncombinatorial contribution to the interaction parameter is significantly larger than is the enthalpic contribution.[32,33] Thus, it seems that an interaction parameter having the correct functionality of temperature and composition may effectively eliminate shortcomings of the original FH lattice theory.

Construction of the Heat of Mixing and Interaction Parameter Function

Several attempts have been made to propose an adequate form for the interaction parameter and a number of expressions were suggested by various investigators.[6,7,10,34–37] Usually, the proposed functions for the interaction parameter can be classified in two types:

(a) It is assumed that χ comprises the temperature-dependent product, $\alpha(T)$, and the composition-dependent, $\beta(\varphi_2)$, terms.[11,38]
(b) A polynomial function of the mixture composition is proposed for χ and the coefficients of the polynomial are assumed to be a particular function of temperature, which, in its general form, can consist of inverse, linear, and logarithmic terms of temperature.[6,7]

According to the original FH lattice theory, in eq. (4), only the inverse temperature functionality was taken into account for χ, but this is an oversimplification, and for actual systems, complementary terms must be considered.[10,39] In the present article, at first, we proceeded by introducing a functionality form for the heat of mixing of two components and then gathered a convenient function for the interaction parameter.

From eqs. (4) and (5), the heat of mixing can be obtained as a function of Δw_{12}:

$$\Delta H^{\text{mix}} = z \Delta w_{12} \varphi_1 \varphi_2 \tag{9}$$

According to the original FH lattice theory, Δw_{12} is assumed to be independent of the temperature and mixture composition and, therefore, the heat of mixing will be independent of the temperature. Furthermore, it has been proven that to achieve a quantitative agreement with an experimental heat-of-mixing data Δw_{12} in eq. (9) also must be a function of the mixture composition.[40,41]

Here, we constructed empirical equations for the heat of mixing and the interaction parameter of polymer mixtures as combined functions of the temperature and mixture composition by introducing the following relation for Δw_{12}:

$$\frac{z \Delta w_{12}}{RT} = A_1 + A_2 T + A_3 \varphi_2 + A_4 \varphi_2 T \tag{10}$$

where the values of A_1–A_4 are constant coefficients and they are independent of the temperature and mixture composition. Substituting for $z\Delta w_{12}$ in eq. (9) gives the heat of mixing as a third-order polynomial with respect to φ_2 with temperature-dependent coefficients:

$$\frac{\Delta H^{\text{mix}}}{R} = -(A_3 + A_4 T)\varphi_2^3 + [(A_3 - A_1) + (A_4 - A_2)T]\varphi_2^2 + (A_1 + A_2 T)\varphi_2 \tag{11}$$

The relation between the heat of mixing and the interaction parameter can be obtained by substituting ΔG^{mix} from eq. (2) in the following equation:

$$\frac{\partial(\Delta G^{\text{mix}}/RT)}{\partial(1/T)} = \frac{\Delta H^{\text{mix}}}{R} \tag{12}$$

and replacing χ_{FH} by a temperature-dependent interaction parameter χ as follows:

$$\Delta H^{\text{mix}} = R\varphi_1\varphi_2\left(\frac{\partial\chi}{\partial(1/T)}\right)_{\varphi_2} \tag{13}$$

By substituting eq. (11) in eq. (13) and integrating the results in the following relation for the interaction parameter,

$$\chi = (A_1 + A_3\varphi_2)(1/T) - (A_2 + A_4\varphi_2)\ln(T) + A_5 \tag{14}$$

where A_5 is the integration constant. Comparing eq. (14) with the original form of the χ parameter by FH, in eq. (4), it is seen that the inverse temperature functionality term is held with a composition dependency.

Phase Stability

By introducing χ from eq. (14) into eq. (2), the following expression for the second derivative of the Gibbs free energy of mixing, the spinodal equation, is obtained:

$$\frac{\partial^2\Delta G^{\text{mix}}}{\partial\varphi_2^2} = \frac{1}{r_1\varphi_1} + \frac{1}{r_2\varphi_2} - 2\chi + 2(1 - 2\varphi_2)\chi' + \varphi_2(1 - 2\varphi_2)\chi'' \tag{15}$$

where χ' and χ'' are the first and second derivatives of χ with respect to the volume fraction , φ_2, at constant temperature:

$$\chi' = \left(\frac{\partial\chi}{\partial\varphi_2}\right)_T \tag{16}$$

$$X'' = \left(\frac{\partial^2\chi}{\partial\varphi_2^2}\right)_T \tag{17}$$

As seen from eq. (14), the χ function is linear with respect to φ_2; thus, from eq. (17), we have $\chi'' = 0$. Later, it will be shown that a linear functionality form for the interaction parameter is sufficient for our heat-of-mixing and spinodal calculations. Substituting the first and second derivatives of the interaction parameter in eq. (15) gives the following expression for the spinodal equation:

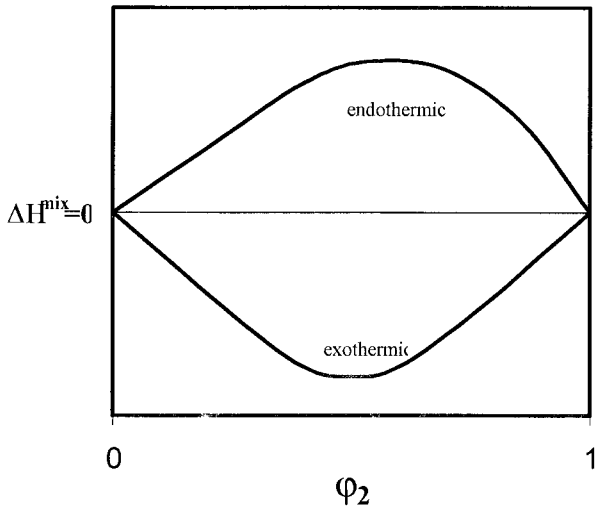

Figure 1 For the exothermic heat-of-mixing curve, $\partial^2(\Delta H^{\text{mix}})/\partial\varphi_2^2$ is positive, and for the endothermic case, $\partial^2(\Delta H^{\text{mix}})/\partial\varphi_2^2$ is negative.

$$\frac{1}{\sum_{i=1}^{2} r_i\varphi_i} - 2[(A_1 - A_3)(1/T) - (A_2 - A_4)\ln(T) + A_5] - 6[A_3/T - A_4\ln(T)]\varphi_2 = 0 \tag{18}$$

Considering the resulting equations for the heat of mixing and the spinodal of the polymer mixtures, eqs. (11) and (18), a qualitative study on the capabilities of these equations is presented here. Usually, the heat-of-mixing curves can be categorized to the exothermic, endothermic, and S-shaped or sigmoidal types. In the exo- and endothermic types, the heat of mixing is, respectively, negative and positive in the entire range of mixture composition at a definite temperature, while in the sigmoidal type, the sign of the ΔH^{mix} function changes between negative and positive values. In other words, at a constant temperature for some compositions, heat is released during the mixing of two components, and for the other compositions, heat is absorbed. It can be shown that eq. (11) can be used to produce all types of the above cases for the heat of mixing. For this purpose, we consider the first and second derivatives of ΔH^{mix} with respect to φ_2 at a constant temperature. In Figure 1, typical forms of exothermic and endothermic heat-of-mixing curves with respect to the mixture composition are depicted. This figure clearly shows that for exothermic and endothermic mixings the second derivative of the

Table I Dependency of Heat of Mixing on Temperature and Composition for Exothermic and Endothermic Mixings ($\alpha = A_3 + A_4T$ and $\beta = A_1 + A_2T$)

	ΔH^{mix}	
	Exothermic	Endothermic
$\partial^2\Delta H^{mix}/\partial\varphi_2^2$	> 0	< 0
$\alpha > 0$	$\varphi_2 > 1/3 - \beta/3\alpha$	$\varphi_2 < 1/3 - \beta/3\alpha$
$\alpha < 0$	$\varphi_2 < 1/3 - \beta/3\alpha$	$\varphi_2 > 1/3 - \beta/3\alpha$

heat of mixing with respect to mixture composition is positive and negative, respectively. According to eq. (11), the second derivative of ΔH^{mix} with respect to φ_2 is obtained as follows:

$$\frac{\partial^2(\Delta H^{mix}/R)}{\partial\varphi_2^2} = -6(A_3 + A_4T)\varphi_2 + 2[(A_3 + A_4T) - (A_1 + A_2T)] \quad (19)$$

Thus, related to the sign of A_4, eq. (19) can produce both exothermic and endothermic heat-of-mixing curves against φ_2. In Table I, the temperature and composition dependency of ΔH^{mix} and the results of the sign determination of the second derivative equation are summarized. For sigmoidal heat-of-mixing curves, two possible states are depicted in Figure 2, where we called them exo–endothermic and endo–exothermic heats of mixing. The third derivative of ΔH^{mix} with respect to φ_2 is negative for exo–endothermic and positive for endo–exothermic mixing. According to eq. (11), the third derivative equation is obtained as follows:

$$\frac{\partial^3(\Delta H^{mix}/R)}{\partial\varphi_2^3} = -6(A_3 + A_4T) \quad (20)$$

Thus, depending on the sign of A_4, we can have exo–endothermic and endo–exothermic mixings. In Table II, the temperature and composition dependency of ΔH^{mix} and the results of the sign determination of the third derivative, eq. (20), are summarized.

It is known that the spinodal curve in a phase diagram determines the phase stability or miscibility region. Various types of spinodals have been observed experimentally for polymer mixtures, such as the lower and upper critical solution temperatures (LCST and UCST) and closed-loop miscibility. According to theoretical predictions, a phase diagram of each polymer mixture must contain both LCST and UCST.[33] Here, we intend to show that eq. (18) can produce all types of phase diagrams. Also, we determined the temperature limits in which these phase diagrams can be observed. Equation (18) is composed of two parts: The first part is related to the combinatorial entropy contribution and is written as follows:

$$\frac{1}{r_1\varphi_1} + \frac{1}{r_2\varphi_2} \quad (21)$$

The second part is related to the energetic effects of mixing, containing enthalpy and noncombinatorial entropy contributions, which can be written as a linear function of composition, φ_2:

$$6\left(A_4 \ln T - \frac{A_3}{T}\right)\varphi_2 - 2[(A_1 - A_3)(1/T) - (A_2 - A_4)\ln(T) + A_5] \quad (22)$$

It is obvious that the combinatorial entropy contribution, eq. (21), always satisfies the phase-stability condition, eq. (1). Therefore, only the second part, eq. (22), can be the source of unstability in the phase diagram. It must be noted that each point on the spinodal curve is obtained by solving

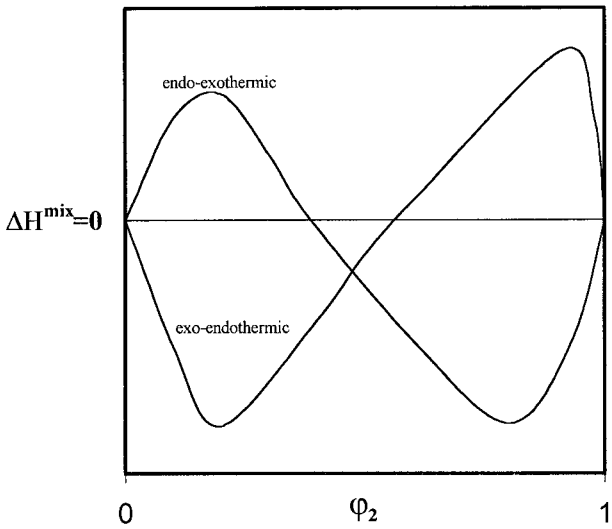

Figure 2 Two possible cases for sigmoidal heat-of-mixing curves. The sign of the third derivative of the heat-of-mixing curve is positive and negative for endo–exothermic and exo–endothermic cases, respectively.

Table II Dependency of Heat of Mixing on Temperature and Composition for Exo–Endo and Endo–Exothermic Mixings ($\alpha = A_3 + A_4T$ and $\beta = A_1 + A_2T$)

	ΔH^{mix}			
	Exo–endothermic		Endo–exothermic	
	Exothermic	Endothermic	Endothermic	Exothermic
φ_2	$< -\beta/\alpha$	$> -\beta/\alpha$	$< -\beta/\alpha$	$> -\beta/\alpha$
$\partial^2\Delta H^{mix}/\partial\varphi_2^2$	> 0	< 0	< 0	> 0
$\partial^3\Delta H^{mix}/\partial\varphi_2^3$	< 0	< 0	> 0	> 0

eq. (18) at a certain temperature. Thus, for a temperature range, eq. (18) must be solved at various temperatures. From eq. (21), it is seen that the combinatorial entropy contribution is independent of the temperature. Therefore, to have a qualitative argument on the presented spinodal equation, it is sufficient to consider the temperature variation of the second part, eq. (22). It is seen that eq. (22) shows a line with a temperature-dependent intercept and slope. The intercept of this line is

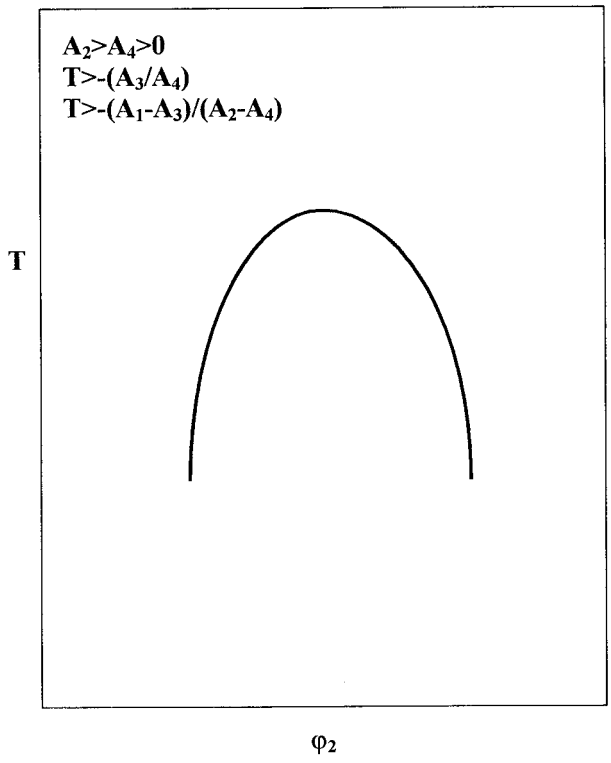

Figure 3 UCST phase diagram and the temperature range at which this type of phase behavior can be observed.

$$i = -2[(A_1 - A_3)(1/T) - (A_2 - A_4)\ln(T) + A_5] \quad (23)$$

A variation of i with respect to the temperature is obtained by differentiating eq. (23) as follows:

$$\frac{\partial i}{\partial T} = 2[(A_1 - A_3) + (A_2 - A_4)T]/T^2 \quad (24)$$

From eq. (24), it is seen that when $A_2 > A_4$, in the temperature range of $T > -[(A_1 - A_3)/(A_2 - A_4)]$, increasing temperature enhances the miscibility of the mixture components, and if $T < -[(A_1 - A_3)/(A_2 - A_4)]$, increasing temperature reduces the miscibility. For the case of $A_2 < A_4$, the temperature ranges for increasing or decreasing miscibility are reversed.

In addition to the intercept of the line of eq. (22), the slope of this line must also be considered for the phase-stability studies. We represent the slope of this line with s:

$$s = 6(A_4 \ln T - A_3/T) \quad (25)$$

The variation of I_2 with respect to the temperature can be obtained by differentiating eq. (25):

$$\left(\frac{\partial s}{\partial T}\right) = (A_3 + A_4T)/T^2 \quad (26)$$

From eq. (26), it is deduced that when $A_4 > 0$ if $T > -(A_3/A_4)$, increasing temperature makes the system more stable, and if $T < -(A_3/A_4)$, increasing temperature reduces the phase stability. For the case of $A_4 < 0$, these temperature ranges are reversed.

It is worth noting that for phase-stability predictions, the temperature variations of i and s,

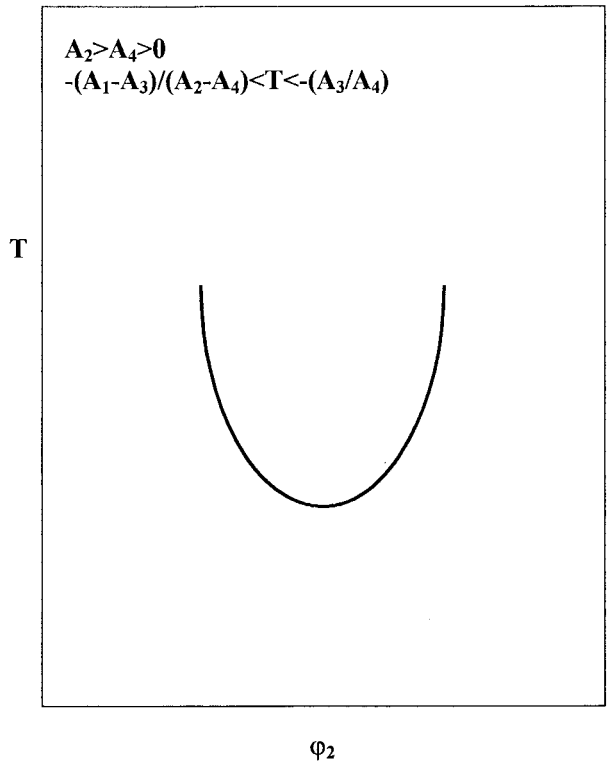

Figure 4 LCST phase diagram and the temperature range at which this type of phase behavior can be observed.

eqs. (24) and (26), must be considered simultaneously. When both of $\partial i/\partial T$ and $\partial s/\partial T$ are positive and initially we have a single-phase mixture, the phase stability of the system will increase with increasing temperature and any immiscibility region will not be appear in the phase diagram. This is consistent with the conditions of $A_2 > A_4 > 0$, $T > -(A_3/A_4)$, and $T > -[(A_1 - A_3)/(A_2 - A_4)]$. For appearing as an UCST-type phase behavior, as seen from Figure 3, we must initially have an immiscible mixture with the above conditions.

For the case of $\partial i/\partial T > 0$ and $\partial s/\partial T < 0$, if initially we have a miscible mixture, increasing temperature can produce an LCST-type phase behavior. This is consistent with the conditions of $A_2 > A_4 > 0$ and $-[(A_1 - A_3)/(A_2 - A_4)] < T < -(A_3/A_4)$, as shown in Figure 4.

If we have a miscible mixture with $\partial i/\partial T < 0$ and $\partial s/\partial T > 0$, then increasing temperature can produce a closed-loop phase behavior. These conditions are consistent with $A_2 > A_4 > 0$ and $-(A_3/A_4) < T < -[(A_1 - A_3)/(A_2 - A_4)]$. Figure 5 shows this type of phase behavior. In closed-loop phase diagrams, the LCST is lower than is the UCST of the mixture. When the LCST of the mixture is higher than the UCST, as seen from Figure 6, we must initially have an immiscible mixture with $\partial i/\partial T > 0$, $\partial s/\partial T < 0$ conditions. Increasing temperature at first causes the system to be miscible. Further increasing the temperature makes the system unstable again. These conditions are consistent with $A_4 > 0$, $A_4 > A_2$, and $-[(A_1 - A_3)/(A_2 - A_4)] < T < -(A_3/A_4)$. It is emphasized again that other combinations of the A_i coefficients can be used to produce various types of phase diagrams and only some typical cases were studied above.

RESULTS AND DISCUSSION

Here, using the proposed expressions for the interaction parameter and enthalpy of mixing presented above, we derive appropriate values for the interaction parameter coefficients of various polymer mixtures, and then we employ these relations for phase stability predictions.

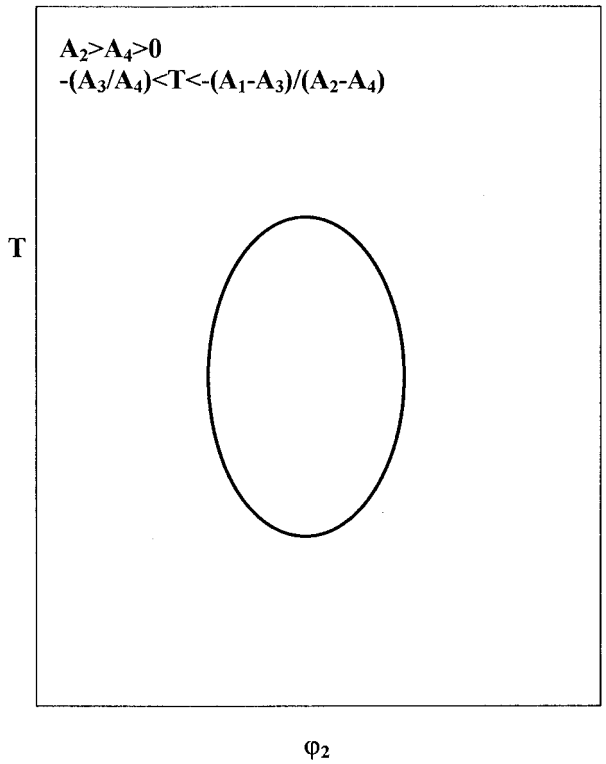

Figure 5 Closed-loop phase diagram and the temperature range at which this type of phase behavior can be observed.

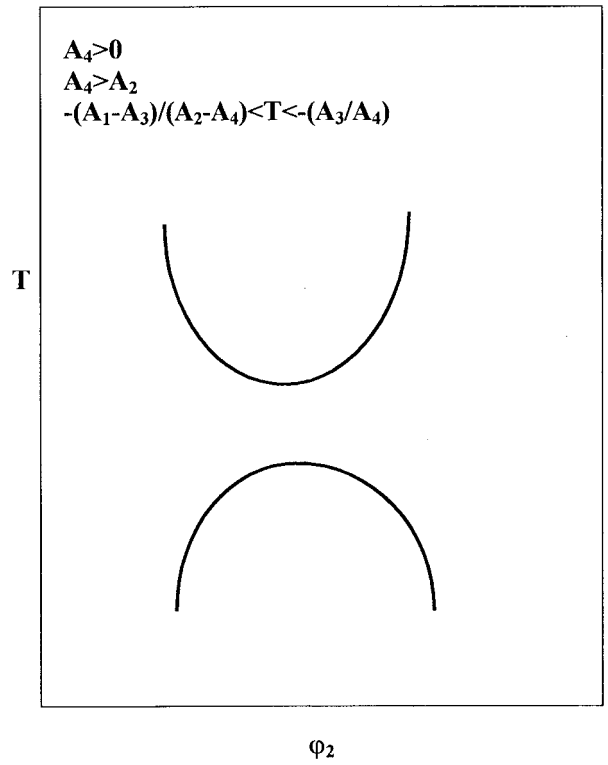

Figure 6 UCST–LCST phase diagram and the temperature range at which this type of phase behavior can be observed.

Polycarbonate (PC)–Poly(ethylene adipate) (PEA) Mixture

For polymer–polymer systems, the calorimetric measurements are difficult because of high viscosity effects.[42] However, the energy change due to mixing is primarily dependent on the energy change associated with change in nearest-neighbor contacts during mixing and much less dependent on molecular lengths.[43] Thus, for these systems, experimental data resulting from analog calorimetric measurements obtained by mixing low molecular weight analogs can be used for the enthalpy of mixing of polymers provided that the values of the heat of mixing per unit volume of the solution are available. Analog calorimetric measurements for study of the heat of mixing of several polymer mixtures were accomplished by Cruz et al.[27] Also, they studied experimentally the temperature variation of ΔH^{mix} for PC and PEA, using diphenyl carbonate (DPhC) and diethyl adipate (DEA) as two reasonable analogs for PC and PEA repeating units. Figure 7 shows the experimental results of analog calorimetric measurements for the mixture of DPhC and DEA at temperatures of 358, 418, and 455 K. As seen from this figure, the mixing process is exothermic and the released heat due to mixing decreases as the temperature of mixing increases. This is one of the characteristics of systems that can exhibit LCST behavior in their phase diagram.

For this system, the interaction parameter coefficients are calculated by fitting eq. (11) to the experimental data of Cruz et al.[27] and they are reported in Table III. By using these coefficients to calculate the heats of mixing, excellent agreement with the experimental data are obtained as shown by the solid lines in Figure 7.

For spinodal calculations, eq. (18) is solved for the phase-stability condition, eq. (1). Values of r_1 and r_2 for two components are obtained by dividing the molar volumes of polymer molecules by a segment volume. Here, an arbitrary segment volume equal to the volume of a carbonate group, —OC(O)O—, in PC repeating units was chosen. The resulting values of r_1 and r_2 depend on the molecular weights of PEA and PC. For low molecular weight analogs of PEA and PC (DEA and DPhC), molar volumes are equal to 175.8 and 188.4 cm^3/mol, respectively, and the volume of a

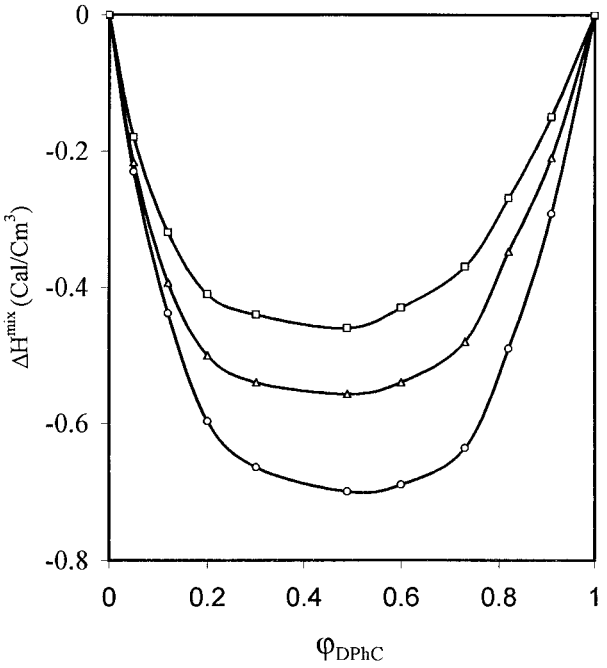

Figure 7 Enthalpy change of mixing for DPhC–DEA mixture. (—) represents the calculated values according to eq. (11). (○) , (△), and (□) represent the experimental data[27] at 358, 418 and 455 K, respectively.

Table III Interaction Parameter Coefficients for Polymer Mixtures According to Eq. (14)

Mixture	A_1	A_2	A_3	A_4	A_5
PC–PEA	−44.402	0.1054	22.5469	−0.0497	0.0025
PVC–PS	7.625	−0.037	44.83	−0.137	0.0121
PVAc–PS	68.900	−0.216	−118.773	0.372	0.0067
EVA Co–CPE	−6.9636	0.01087	−1.4771	0.0041	−0.0150

carbonate group is equal to 31.4 cm^3/mol. Thus, values of r_1 and r_2 are equal to 5.6 and 6, respectively (PC is the second component). Solving eq. (18) for these values of r_1 and r_2 satisfies the phase-stability condition, eq. (1), in all composition ranges, that is, the DPhC and DEA mixture is miscible in the temperature range of 280–350 K as indicated by the experimental observations of Cruz et al.[27] Using higher molecular weight components corresponding to $r_1 = r_2 = 20$ leads to a narrow immiscibility region in this mixture. In Figure 8, the results of spinodal calculations are reported for this mixture. Prediction of an immiscible phase region in Figure 8 could be attributed to the high molecular weights of polymers, as was pointed out by other workers.[26]

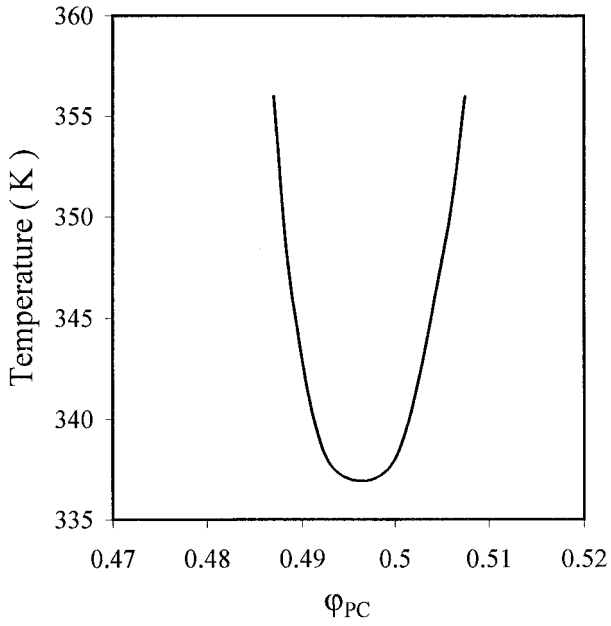

Figure 8 Predicted miscibility boundaries for PC–PEA mixture according to eq. (18). The interaction parameter coefficients are given in Table III.

Poly(vinyl chloride) (PVC)–Polystyrene (PS) Mixture

For this system, we measured the heat of mixing values, using low molecular weight analogs of dichloropentane (DCP) and ethylbenzene (EB) for PVC and PS, respectively. The measured values are related to two temperatures of 27 and 37°C in the entire composition range and they are shown in Figure 9. The method of the experiments was described elsewhere.[44] As seen from Figure 9, mixing of DCP and EB is exothermic and the released heat of mixing increases with increasing temperature. It is well known that increasing temperature reduces the density of both the mixture and the pure components. Thus, the strength

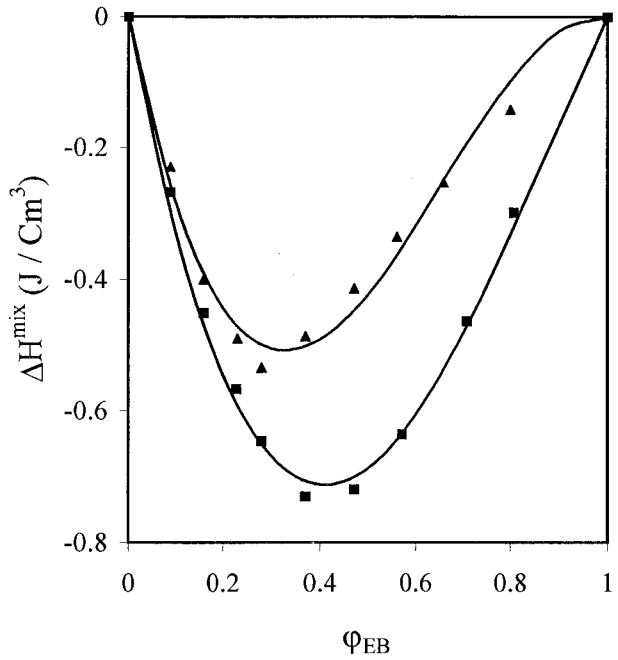

Figure 9 Experimental heats of mixing for the mixture of DCP–EB at two temperatures of (▲) 27 and (■) 37°C. Solid curves are the results of calculations according to eq. (11).

of the molecular interactions would be reduced because of increasing distances between the interacting molecules. Increasing the released heat of mixing at elevated temperatures for the EB/DCP mixture is maybe due to that interactions of molecules in a pure-component state are more sensitive to temperature than are the interactions among the dissimilar molecules in the mixture.

To obtain the coefficients of the empirical heat of mixing equation, which was introduced in the previous section, we used the experimental results with a least-mean-square data-fitting method. The values of these coefficients are given in Table III. In Figure 9, heats of mixing at two temperatures of 27 and 37°C calculated by eq. (11) are depicted by solid curves. In Figure 10, the results of spinodal calculations according to eq. (18) for this mixture are presented. As seen from this figure, the spinodal curves are dependent on the values of r_1 and r_2 for the two components. Experimental observations showed that PVC and PS are immiscible and this is in agreement with the calculated results for r_1 and $r_2 > 20$. Another important point about this mixture is that for low molecular weight analogs of PVC and PS with r_1 = 2 and r_2 = 1.5 an UCST–LCST-type phase behavior is obtained. For explaining this phenomenon, some reasons can be established: Low molecular weight analogs like EB or DCP have spatial freedom to align with each other and they interact in any desired state. Thus, they can produce molecular complexes, maybe due to hydrogen-bonding formation between the π electron of the aromatic and the α-hydrogen of DCP[45] or a dipole-induced dipole interaction,[46] while macromolecules of PS and PVC have long chains that considerably reduce the free motion of their repeating units and they cannot completely interact to realize the exothermic mixing.

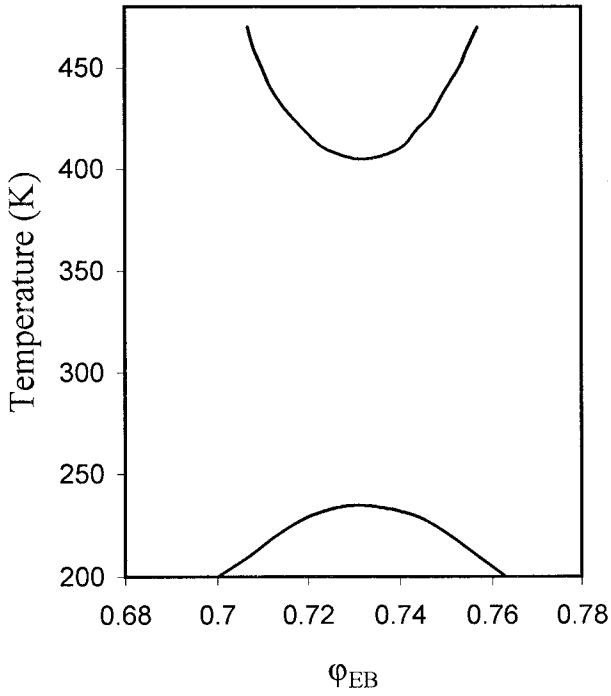

Figure 10 Predicted miscibility boundaries for PVC–PS mixture according to eq. (18). The interaction parameter coefficients are given in Table III.

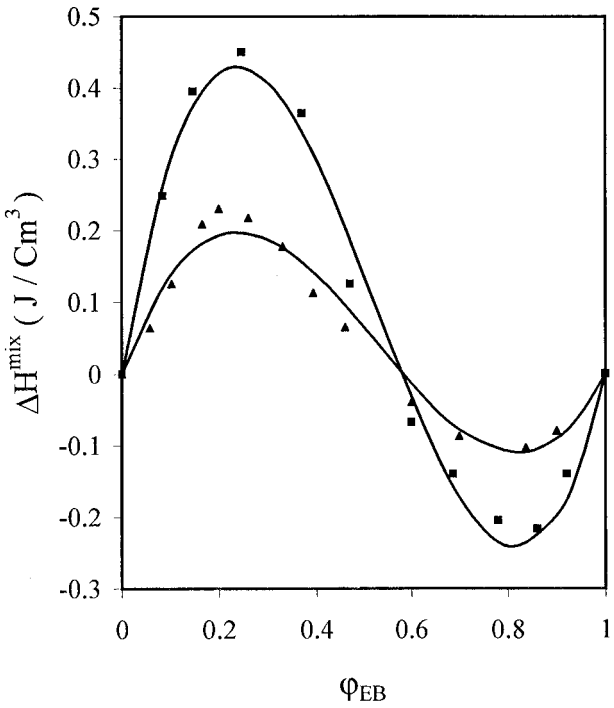

Figure 11 Experimental heats of mixing for the mixture of EA–EB at two temperatures of (▲) 27 and (■) 37°C. Solid curves are the results of calculations according to eq. (11).

Poly(vinyl acetate) (PVAc)–PS Mixture

Heat of mixing values for this system were measured by the authors[44] using low molecular weight analogs of EA and EB for PVAc and PS, respectively. The results of the experiments are shown in Figure 11. It is seen that the sign of ΔH^{mix} switches between the positive and negative values and the released or absorbed heat in-

creases with increasing temperature. This type of ΔH^{mix} is called the S-shaped or sigmoidal heat-of-mixing curve and it is observed for some mixtures of ketons with chlorinated compounds[47] and chlorinated paraffins with oligomeric poly(methyl metacrylate).[48] This phenomenon is consistent with the UCST–LCST phase behavior.[37] For spinodal calculations according to eq. (18), we used the values of the A_i coefficients which were determined from the experimental heat-of-mixing data. These values are given in Table III. The results of spinodal calculations with $r_1 = 1.1$ for PVAc and $r_2 = 1.3$ for PS are shown with solid curves in Figure 12. In actual cases, values of r_1 and r_2 for polymers are much greater than are their values for the low molecular weight analogs, and for a typical case of $r_1 = r_2 = 100$, the results of spinodal calculations are shown with dashed curves in Figure 12. To our knowledge about this mixture, only the phase behavior of PS with alkyl acetates, such as methyl acetate, ethyl acetate and *tert*-butyl acetate, exists in the literature.[49]

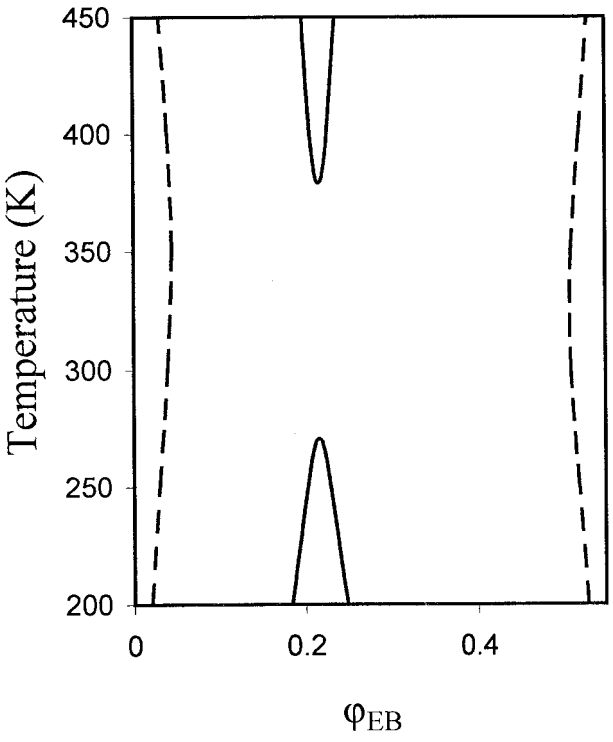

Figure 12 Predicted miscibility boundaries for PVAc–PS mixture according to eq. (18). Solid curves are the results of calculations with $r_1 = 1.1$ and $r_2 = 1.3$ and dashed curves show the results of calculations with $r_1 = r_2 = 100$. The interaction parameter coefficients are given in Table III.

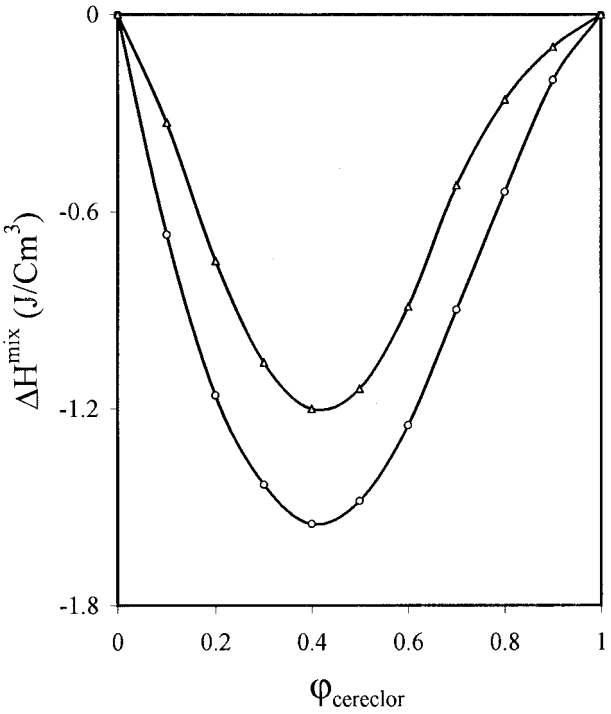

Figure 13 Enthalpy change of mixing for the mixture of 2OA–C52. (—) represents the calculated values according to eq. (11). (○) and (△) are the experimental data[24] for temperatures 337.5 and 357.5 K, respectively.

All these mixtures show the UCST–LCST-type phase behavior, which is in agreement with the results of our spinodal calculatiuons for low molecular weights of PVAc and PS.

Ethylene Vinyl Acetate Copolymer (EVA Co)–Chlorinated Polyethylene (CPE)

For this system, Walsh et al.[26] recommended using an oligomer mixture of cereclor-52 (C52), a commercial chlorinated paraffin, with 2-octyl acetate (2OA) as low molecular weight analogs for EVA Co and CPE, respectively. Experimental values for the heat of mixing of C52 + 2OA at temperatures of 337.5, 346, and 357.5 K are shown in Figure 13. Using the model proposed in this work, the interaction parameter coefficients are calculated and reported in Table III. The results of the calculations for the heat of mixing based on the fitted interaction parameter coefficients are also shown, as solid curves, in Figure 13. The good agreement between the results of the calculations and the reported experimental values is another

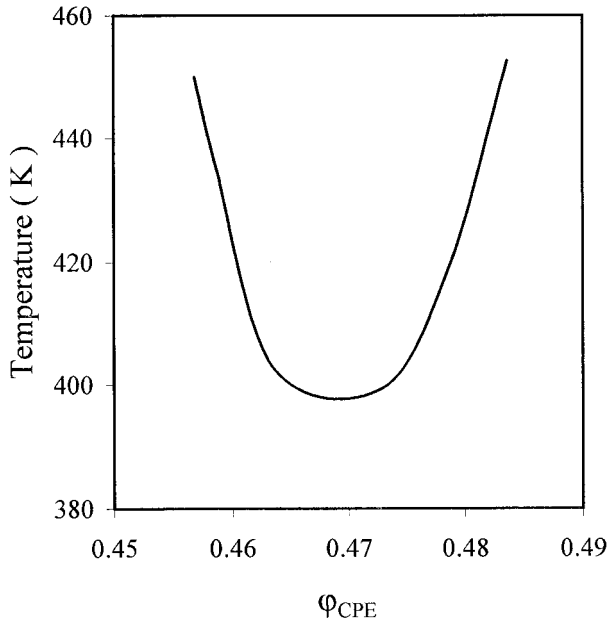

Figure 14 Predicted miscibility boundaries for the EVA copolymer–CPE mixture according to eq. (18). The interaction parameter coefficients are given in Table III.

indication of the appropriateness of the derived functionality for the interaction parameter. Values of $r_1 = 23.1$ and $r_2 = 20$ are used for phase-stability predictions. The calculated spinodal curve for this polymer mixture is shown in Figure 14, which indicates the appearance of phase separation with increasing temperature, according to Walsh et al.[26] This is due to the noncombinatorial entropy contribution.

CONCLUSIONS

A general approach for obtaining the enthalpy change upon mixing and predicting the phase stability for polymer–polymer mixtures was presented. To achieve this, an appropriate temperature and composition-dependent expression for the interaction parameter was proposed. The coefficients of the proposed interaction parameter expression are evaluated from the experimental data for several mixtures. Good agreement between the calculated results and experimental data for the enthalpy of mixing was obtained. Also, it was demonstrated that the proposed model has the capability of predicting spinodal curves and phase-stability conditions for any kind of polymer mixture irrespective of the kind of polymers in the systems. The applicability of the present model for mixtures containing polymer chains with different functional groups indicated that it can be used for mixtures with both physical interactions, such as dispersion forces, and chemical associations that arose from hydrogen bonding.

REFERENCES

1. Flory, P. J. J Chem Phys 1942, 10, 51.
2. Flory, P. J. J Chem Phys 1944, 12, 425.
3. Flory, P. J. J Chem Phys 1946, 14, 49.
4. Huggins, M. L. Ann NY Acad Sci 1942, 41, 1.
5. Huggins, M. L. J Phys Chem 1942, 46, 151.
6. Koningsveld, R.; Macknight W. J. Polym Int 1997, 44, 356.
7. Soenen, H. S.; Moerkerke, R.; Berghmans, H.; Koningsveld, R.; Dusek, K.; Solc, K. Macromolecules 1997, 30, 410.
8. Painter, P. C.; Veytsman, B.; Kumar, S.; Shenoy, S.; Graf, J. F.; Xu, Y.; Coleman, M. M. Macromolecules 1997, 30, 932.
9. Painter, P. C.; Lennart, P. B.; Veytsman, B.; Coleman, M. M. Macromolecules 1997, 30, 7529.
10. Gomez, C. M.; Verdejo, E.; Figueruelo, J. E.; Compas, A.; Soria, V. Polymer 1995, 36, 1487.
11. Qian, C.; Mumby, S. J.; Eichinger, B. Macromolecules 1991, 24, 1655.
12. Sanchez, I. C.; Lacombe, R. H. J Phys Chem 1976, 80, 2352.
13. Eichinger, B. E.; Flory, P. J. Trans Faraday Soc 1968, 64, 2035.
14. Flory, P. J.; Orwoll, R. A.; Vrij, A. J Am Chem Soc 1964, 86, 3507.
15. Panayiotou, C.; Sanchez, I. C. J Phys Chem 1991, 95, 10090.
16. Graf, J. F.; Coleman, M. M.; Painter, P. C. J Phys Chem 1991, 95, 6710.
17. Panayiotou, C. Macromolecules 1987, 20, 861.
18. Patterson, D. Rubb Chem Technol 1967, 40, 1.
19. Hoy, K. L. J Paint Technol 1970, 42, 76.
20. Barton, A. F. Handbook of Solubility Parameters and Other Cohesion Parameters; CRC: Boca Raton, FL, 1983.
21. Barton, A. F. Handbook of Polymer–Liquid Interaction Parameters and Solubility Parameters; CRC: Boca Raton, FL, 1990.
22. Brandrup, J.; Immergut, E. H. Polymer Handbook, 3rd ed.; Wiley: New York, 1989.
23. Orwoll, R. J. Rubb Chem Technol 1977, 452, 50.
24. Olabisi, O.; Robenson, L. M.; Shaw, M. T. Polymer Polymer Miscibility; Academic: London, 1979.

25. Flory, P. J. Principles of Polymer Chemistry; Cornell University: Ithaca, NY, London, 1953.
26. Walsh, D. J.; Higgins, J. S.; Rostami, Sh.; Weeraperuma, K. Macromolecules 1983, 16, 391.
27. Cruz, C. A.; Barlow, J. W.; Paul, D. R. Macromolecules 1979, 12, 726.
28. Ziaee, S.; Paul, D. R. J Polym Sci Part B Polym Phys 1997, 35, 489.
29. Cruz, C. A.; Paul, D. R. Macromolecules 1989, 22, 1289.
30. Kizhnyaev, V. N.; Gorkovenko, O. P.; Bazhenov, D. N.; Smirnov, A. I. Polym Sci Ser A 1997, 39, 579.
31. Safronov, A. P.; Suvorova, A. I.; Koroleva, E. V.; Maskalyunaite, O. E. Polym Sci Ser A 1997, 39, 1322.
32. Schultz, G. V.; Doll, H. Z Electrochem 1952, 52, 248.
33. Tager, A. A. Physical Chemistry of Polymers; Khimiya: Moscow, 1978.
34. Nose, T. Polymer, 1995, 36, 2243.
35. Ahn, J. H.; Kang, C. K.; Zin, W. C. Eur Polym J 1997, 33, 1113.
36. Hadj-Hamou, A. S.; Habi, A.; Djadoun, S. Eur Polym J 1997, 33,1105.
37. Solc, K.; Koningsveld, R. J Phys Chem 1992, 96, 4056.
38. Kamide, K.; Matsuda, S.; Saito, M. Polym J 1985, 17, 1013.
39. Cimmino, S.; Karasz, F. E.; Macknight, W. J. J Polym Sci Part B Polym Phys 1992, 30, 49.
40. Coleman, M. M.; Graf, J. F.; Painter, P. C. Specific Interactions and the Miscibility of Polymer Blends; Technomic: Lancaster, 1991.
41. Kurata, M. Thermodynamics of Polymer Solutions; Harwood: New York, 1982.
42. Paul, D. R.; Barlow, J. W.; Keskkula, H. In Mark, H.; Bikales, N. M.; Overborger, C. G.; Menges, G., Eds.; Encyclopedia of Polymer Science and Engineering, 2nd ed.; Vol. 12, p 398.
43. Svoboda, P.; Kressler, J.; Ougizawa, T.; Inoue, T.; Ozutsumi, K. Macromolecules 1997, 30, 1973.
44. Taimoori, M.; Modarress, H.; Saboury, B. A.; Moosavi-Movahedi, A. A., submitted for publication in J Polym Eng Sci.
45. Abello, L. J Chem Phys 1973, 70, 1355.
46. Schneider, W. G. J Phys Chem 1962, 66, 2653.
47. Etxeberria, A.; Iriarte, M.; Iruin, J. J. Macromolecules 1995, 28, 589.
48. Walsh, D. J.; Higgins, J. C.; Zhikuan, C. Polymer 1982, 23, 336.
49. Bae, Y. C.; Shim, J. J.; Soane, D. S.; Prausnitz, J. M. J Appl Polym Sci 47, 1193. 1993.